

Functionalization of Gold Nanoparticles by Iron(III) Complexes Derived from Schiff Base Ligands

Cédric R. Mayer,^[a] Gregory Cucchiaro,^[a] Josseline Jullien,^[a] Frédéric Dumur,^[a]
Jérôme Marrot,^[a] Eddy Dumas,^{*[a]} and Francis Sécheresse^[a]

Keywords: Gold nanoparticles / Schiff base ligands / Iron / Isothiocyanate

A series of iron(III) complexes derived from a variety of pentadentate Schiff base ligands, namely salten [H₂salten = bis(3-salicylideneaminopropyl)amine] derivatives, have been synthesized and further used to stabilize and functionalize gold nanoparticles (Au-NPs). The iron complexes have been specifically designed to interact with the Au-NPs through an ambidentate thiocyanate ligand or through a pendant thiol group carried by the salten derivative ligand. The gold nanocomposites have been synthesized either by direct reduction

of Au^{III} in the presence of iron complexes or by coordination chemistry on prefunctionalized gold nanoparticles; in the latter case Au-NPs bearing pendant empty salten cages have been treated with Fe^{III} to generate the iron complexes. Steric and electrostatic repulsions have been tuned to obtain stable colloidal solutions or to induce the precipitation of the gold nanocomposites.

(© Wiley-VCH Verlag GmbH & Co. KGaA, 69451 Weinheim, Germany, 2008)

Introduction

Recent advances in the preparation of stable noble metal nanoparticles (NPs) that exhibit tuneable shapes and a high degree of size monodispersity have contributed to the rapid development of nanoscience. The ability to synthesize nanocomposites in aqueous medium or in organic solvents led to the modification of the surface of metal NPs by a large variety of stabilizing and functionalizing agents. Among these are ionic liquids that can act as template, stabilizer and solvent,^[1] dendrimers^[2] or biomolecules.^[3] Comparatively, the interaction of metal complexes with metal NPs has been much less investigated.^[4] Metal ions have been used, for example, to trigger the assembly/disassembly of metal NPs bearing adapted functional pendant groups such as carboxylic acid,^[5,6] phenol,^[7] bipyridine^[8] or terpyridine.^[9] Such metal-ion-mediated assembly/disassembly of metal NPs has been elegantly employed for the selective colorimetric sensing of metal ions.^[5,7,8] Among the various metal complexes anchored on metal NPs, ruthenium complexes^[10–12] and ferrocene derivatives^[13] have been the most employed. The aim was to study the influence of the metal NPs on the photophysical and/or electrochemical properties of these metal complexes. Astruc et al. also showed that Au-NPs functionalized with electroactive ferrocenyl derivatives could be used for the selective recognition of adenosine-5'-

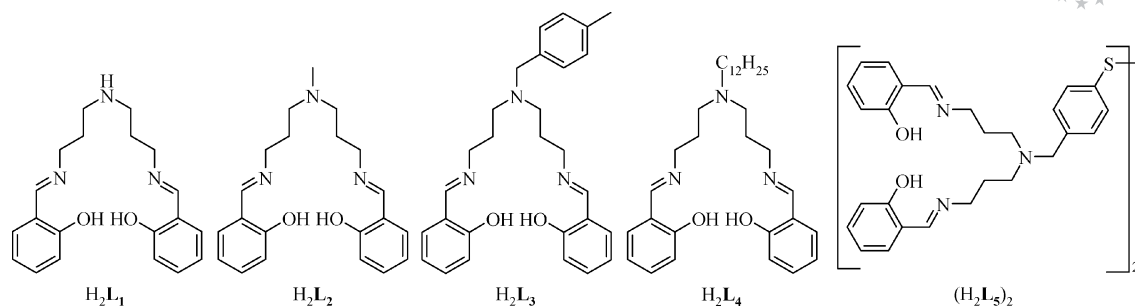
triphosphate, H₂PO₄⁻ and HSO₄⁻ anions.^[14] If the interaction of ferrocene derivatives with metal NPs has been well-documented, the stabilization of metal NPs with other types of iron complexes has only been scarcely described: Au-NPs have been modified with pentacyanoferrates, through suitable bridging ligands,^[15,16] and with electroactive Prussian blue.^[17] Recently, Au-NPs functionalized by the iron cluster [Fe₄(μ₃-CO)₄(η⁵-C₅H₅)₃{η⁵-C₅H₄CONH-(CH₂)₁₁SH}] have also been used for the redox recognition of oxo-anions.^[18]

On the other hand, pentadentate Schiff base ligands such as salten²⁻ [H₂salten = bis(3-salicylideneaminopropyl)amine] and its derivatives have been extensively used to isolate transition-metal complexes with specific magnetic properties. For example, salten²⁻ was used for the synthesis of the first non-heme diiron complex singly bridged by a hydroxy group,^[19] and mesalten²⁻ [H₂mesalten = bis(3-salicylideneaminopropyl)methylamine] was employed as blocking ligand to synthesize tetranuclear,^[20] pentanuclear^[21] and heptanuclear^[21,22] Prussian-blue-like molecules. A series of iron(III) compounds with the general formula [(salten)Fe(L)]ⁿ⁺ (*n* = 0, 1) has also been characterized. The choice of the ligand L occupying the sixth position around the sixfold-coordinated iron centre is crucial to obtain light-induced or thermally induced spin change in these complexes.^[23–26] The magnetic properties of spin-crossover dinuclear iron(III) complexes with the general formula [(salten)Fe(L')Fe(salten)]²⁺ have also been studied.^[27]

We have recently reported the functionalization of noble metal NPs with fully conjugated (polypyridyl)ruthenium complexes.^[11,28,29] The aim of this project is to induce a synergistic effect between the intrinsic properties of the two

[a] Institut Lavoisier de Versailles, UMR 8180, Université de Versailles, 45 Avenue des Etats-Unis, 78035 Versailles, France
Fax: +33-1-39254381
E-mail: dumas@chimie.uvsq.fr

Supporting information for this article is available on the WWW under <http://www.eurjic.org> or from the author.



Scheme 1. Ligands investigated in this work.

components of these nanocomposites. (Polypyridyl)ruthenium complexes were initially chosen owing to their well-known optical and electrochemical properties while the fully π -conjugated bridge between the ruthenium centre and the metal NP was introduced in order to facilitate electronic transfers. Besides, this family of complexes can be “straightforwardly” modified with a variety of functional pendant groups such as thiol,^[12] pyridine,^[11,28] phenanthroline,^[11,28] thiophene^[11] and mercaptopyridine^[29] to ensure their interaction with the metal NPs. In the present work, we extended this approach to another class of metal complexes, namely salten derivatives, Schiff base complexes of iron(III). Three new complexes with the general formula $[(L)Fe(NCS)]$, where L denotes the pentadentate ligands salten²⁻ (**L**₁), mesalten²⁻ (**L**₂), tolylsalten²⁻ (**L**₃) [**H**₂tolylsalten = bis(3-salicylideneaminopropyl)tolylamine], have been structurally characterized and further used to functionalize gold NPs. The anchoring point of the complexes with the metal surface was ensured by the pendant sulfur atom of the ambidentate thiocyanate ligand. The complex [(dodecanesalten)Fe(NCS)], where **H**₂dodecanesalten (**H**₂**L**₄) = bis(3-salicylideneaminopropyl)dodecanamine, has then been employed to enhance the stability of the nanocomposites because of the presence of the long alkyl chain. The fifth salten derivative ligand studied in this work, tolylthiolsalten²⁻ [(**H**₂**L**₅)₂] [**H**₂tolylthiolsalten = bis(3-salicylideneaminopropyl)-p-tolylthiolamine], was specifically designed to strengthen the interaction of the iron complex with the metal surface. **L**₅ proved to be an effective reagent for the synthesis of Au-NPs. The thiol end group of the heteroditopic ligand **L**₅ ensured the interaction with the gold surface by leaving the salten²⁻ pendant group available to complex Fe³⁺ ions (Scheme 1).

Results and Discussion

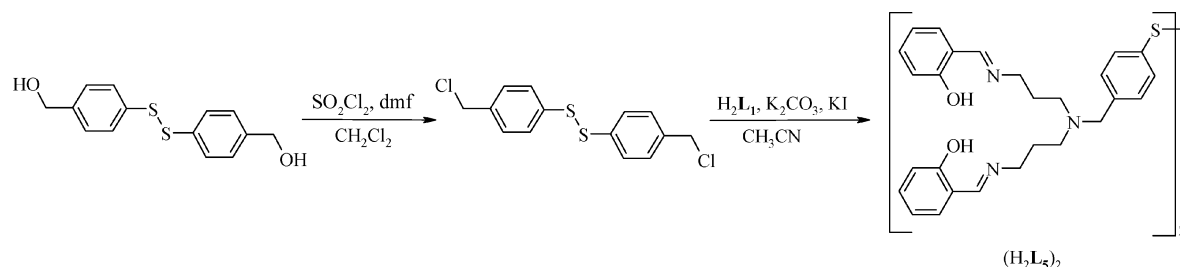
Syntheses of the Ligands and Iron Complexes

Schiff base ligands **H**₂**L**₁ and **H**₂**L**₂ were prepared according to procedures previously reported.^[20,26] *N*-substituted Schiff base ligands **H**₂**L**₃ and **H**₂**L**₄ were synthesized by treating **H**₂**L**₁ with 4-methylbenzyl bromide and bromododecane, respectively. The ligand **H**₂**L**₅ was isolated in its disulfide form in two steps, as summarized in Scheme 2. 4,4'-dithiobis(benzyl chloride) was prepared from 4,4'-dithiobis(benzyl alcohol) in the first step, and was then treated in the second step with two equivalents of **H**₂**L**₁ to afford (**H**₂**L**₅)₂. The disulfide bond was generated to protect the thiol function during the second step. Disulfide ligands have already been successfully used to stabilize metal NPs, undergoing in situ reduction into two thiols capping the NPs,^[30] and in place-exchange reactions on metal NPs.^[31]

All the iron complexes were obtained by following the same procedure: An ethanol solution of one equivalent of the appropriate salten derivative ligand and two equivalents sodium methoxide was slowly added to an ethanol solution containing one equivalent iron(III) nitrate and excess ammonium thiocyanate. The ligands and iron complexes were characterized by using electrospray ionization mass spectrometry, IR and ¹H- and ¹³C NMR spectroscopy (see Experimental Section and Supporting Information).

Structures of the Iron Complexes

Suitable crystals for single-crystal X-ray diffraction analysis were obtained for [(**L**₁)Fe(NCS)] (**1**), [(**L**₂)Fe(NCS)] (**2**) and [(**L**₃)Fe(NCS)] (**3**). The molecular structures of the

Scheme 2. Synthetic pathway of (**H**₂**L**₅)₂.

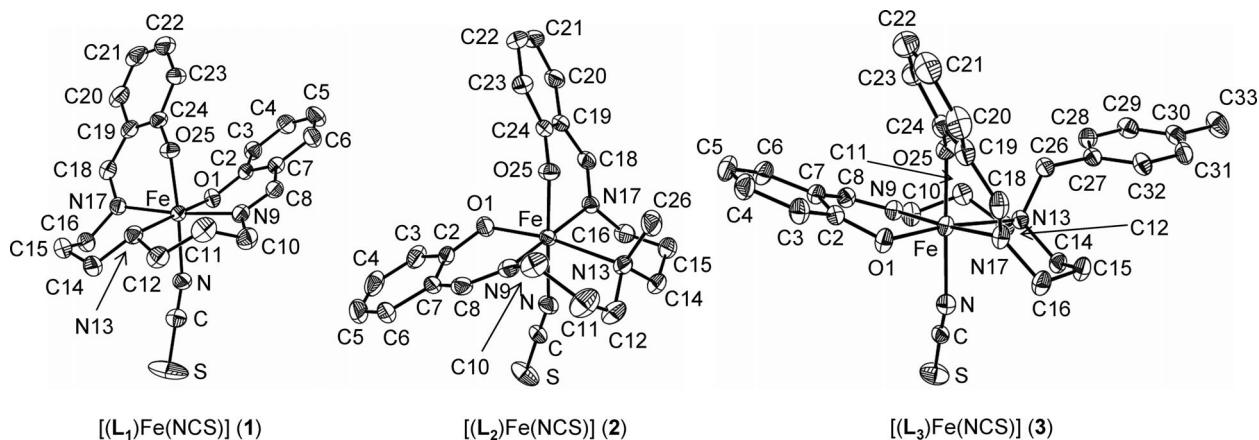


Figure 1. ORTEP representation (ellipsoids drawn at the 30% probability level) of the molecular structures of $[(L_1)Fe(NCS)]$ (**1**), $[(L_2)Fe(NCS)]$ (**2**) and $[(L_3)Fe(NCS)]$ (**3**). Hydrogen atoms were omitted for clarity.

three complexes are shown in Figure 1. Selected bond lengths and angles are given in Table 1. In the three complexes, the iron atom adopts a highly distorted octahedral geometry comprising three nitrogen atoms (one N_{amino} and two N_{imino}) and two oxygen atoms ($O_{\text{phenolato}}$) of the pentadentate salten ligand. One isothiocyanato ligand completes the coordination sphere to give a neutral molecule. In the monoiron complexes of general formula $[(\text{salten-derivative})Fe(L)]$ described in the literature, the ligand L is *trans* either to the amino group [$L = 4\text{-styrylpyridine}$,^[24] 1-(pyridine-4-yl)-2-(*N*-methylpyrrol-2-yl)ethane,^[25] 4-methylpyridine,^[26] 4-aminopyridine,^[32] 3,4-dimethylpyridine^[33]] or to one of the phenolato groups ($L = \text{chloride}$,^[21] salicylaldehyde^[34]) of the salten-derivative ligand. The relative position of L is crucial, as the steric hindrance induced by the two phenyl rings of the salten ligand around ligand L is increased in the former case relative to the latter case. In complexes **1**, **2** and **3**, the isothiocyanato ligand is *trans* to a phenolato group, hence making the pendant S atom of the isothiocyanato ligand fully available to interact with a metal surface. A closer examination of the molecular structures reveals that the steric hindrance around the isothiocyanato ligand is increased in **2**, relative to **1** and **3**, because of the orientation of the phenyl ring of the phenolato group *cis* to NCS^- (Figure 1).

Table 1. Selected bond lengths [\AA] and angles [$^\circ$] in $[(L_1)Fe(NCS)]$ (**1**), $[(L_2)Fe(NCS)]$ (**2**) and $[(L_3)Fe(NCS)]$ (**3**).

	$[(L_1)Fe(NCS)]$	$[(L_2)Fe(NCS)]$	$[(L_3)Fe(NCS)]$
Fe–O1	1.9242(16)	1.9259(16)	1.9161(13)
Fe–O25	1.9368(18)	1.9346(15)	1.9319(14)
Fe–N(CS)	2.061(2)	2.0985(19)	2.0881(18)
Fe–N17 _{imino}	2.108(2)	2.0829(18)	2.0827(16)
Fe–N9 _{imino}	2.126(2)	2.0938(19)	2.1090(15)
Fe–N13 _{amino}	2.233(2)	2.2647(18)	2.3113(15)
Fe–N–C(S)	166.9(3)	161.5(2)	152.62(17)
N–C–S	179.1(3)	179.0(2)	178.47(19)

It is now well established that, in ferric Schiff base complexes (among others), the iron–ligand distances are noticeably affected by the spin state of the iron(III) centre.^[24,35,36]

The average iron–ligand bond lengths of 2.065, 2.067 and 2.073 \AA for **1**, **2** and **3**, respectively, are consistent with high-spin complexes.^[36] The Fe– $O_{\text{phenolato}}$, Fe– N_{imino} and Fe– N_{amino} distances in **1**, **2** and **3** are well within the ranges expected for a high-spin iron(III) centre.^[36] Magnetic measurements confirmed the magnetic properties inferred from the geometrical characteristics of the complexes (Figure S1, Supporting Information). The only two significant structural differences between the three complexes are the Fe– N_{amino} distance, indeed affected by the nature of the R group in the $N_{\text{amino}}\text{-R}$ -substituted salten ligand (R being $-\text{H}$, $-\text{CH}_3$ and $-\text{CH}_2\text{-C}_6\text{H}_4\text{-CH}_3$ in **1**, **2** and **3**, respectively), and the slightly bent Fe–N–C(S) angle [166.9(3), 161.5(2) and 152.6(2) in **1**, **2** and **3**, respectively]. The NCS^- ligands are almost linear in all three complexes.

Preliminary Investigations: Preparation and Characterization of Au-NPs with $[(L_1)Fe(NCS)]$ (**1**), $[(L_2)Fe(NCS)]$ (**2**) and $[(L_3)Fe(NCS)]$ (**3**) as Capping Agents

NCS^- was inserted in the coordination sphere of the iron centre of **1**, **2** and **3** to ensure the grafting of the metal complex on the metal NP. NCS^- has already been used as (co)adsorbed probe for Surface Enhanced Raman Spectroscopy (SERS) characterization of various metal NPs,^[37] but the isothiocyanato group has only been scarcely employed as anchoring moiety for the functionalization of metal NPs either with organic dyes^[38] or with a ruthenium complex.^[39] The molecular structures of **1**, **2** and **3** had a similar geometry around the iron(III) centre and also showed a limited steric hindrance of the salten derivative around the isothiocyanato ligand. Given such favourable geometric characteristics, the three complexes were used as stabilizing agents for the synthesis of metal NPs. Very similar findings were obtained with the three complexes and only the results obtained with **1** are presented in this article. The direct syntheses, in which Au^{III} was reduced in the presence of **1** by excess NaBH_4 , were performed in dmf (see Experimental Section). The syntheses were realized by using various $[\text{Au}^{\text{III}}]/[\mathbf{1}]$ ratios between 0.25 and 6. The sta-

bility of the colloidal solutions and the size and shape of the final nanocomposites were not noticeably affected by this ratio. The colloidal solutions were first studied by UV/Vis spectroscopy. After reduction of Au^{III} with NaBH₄, a maximum absorption peak was observed in the visible region at ca. 520 nm. The study was complicated by the presence of the LMCT band of **1** centred at 513 nm and therefore located in the region expected for the SPR (surface plasmon resonance) band of Au-NPs with a diameter of few nanometres. Consequently, the peak at ca. 520 nm was attributed to the sum of the absorption of the Au-NPs (SPR) and the LMCT of **1**, explaining the slight redshift and the slight increase in the intensity of the peak relative to that of the peak of pure **1** in the same conditions (Figure S2, Supporting Information). The presence of Au-NPs was further confirmed by TEM. TEM analysis showed that Au-NPs polydisperse in size (between 3 and 12 nm) and in shape were formed, but they aggregated or fused in a few minutes to give larger particles and aggregates. Aggregates of several tens of nanometres were observed after 4 min.

These first results clearly show that iron complexes **1**, **2** and **3** are not adapted for the functionalization of Au nanocomposites. At first, the iron complexes perfectly play their role of stabilizing agent as they clearly prevent further growth of Au-NPs. Nevertheless, the stability of the Au nanocomposites is only partial, as the Au-NPs rapidly aggregate and fuse. Several phenomena could explain the rapid aggregation of the NPs: (i) A weak interaction of the pendant thiocyanato ligand with the gold surface, leading to rapid leaching of the iron complexes. (ii) A rupture of the SCN–Fe bond resulting from the interaction of the thiocyanato ligand with the gold surface. Such behaviour has already been observed with the labile [Fe(CN)₅(2MPy)]³⁻ complex (2MPy = 2-mercaptopyridine) that acted as a source delivering 2MPy to the Au-NPs.^[15] (iii) The absence of sufficient steric repulsion by the surface-bonded metal complexes to ensure dispersion stability. (iv) The absence of electrostatic repulsion preventing aggregation of the nanocomposites, as the capping agents are neutral iron complexes. The first two assumptions have been ruled out by EDX analyses of the repeatedly washed precipitates. These analyses unambiguously showed the presence of iron complexes in these aggregates. We therefore decided to modify the iron complexes either to enhance the steric repulsion between nanocomposites or to generate an electrostatic repulsion induced by charged iron complexes.

Functionalization of Au-NPs by [(L₄)Fe(NCS)]

Capping agents bearing a long alkyl chain have often been used to stabilize metal NPs. The role of this long alkyl chain is to induce steric repulsion against the van der Waals attraction between metal NPs and therefore to prevent them from further growth and aggregation. Such an approach was elegantly employed for the well-known Brust–Schiffrin method.^[40] The ligand H₂L₄ was specifically designed to carry a pendant dodecyl chain, grafted on the N_{amino} atom

of the salten ligand. Stable colloidal solutions of Au-NPs functionalized by [(L₄)Fe(NCS)] (**4**) were obtained, in dmf, by reduction of HAuCl₄ with excess NaBH₄ in the presence of **4** (see Experimental Section). Excess iron complex was removed by repeated centrifugations of the colloidal solutions and redispersion of the nanocomposites in dmf. The peak observed at ca. 520 nm in the absorption spectrum of the colloidal solution was associated with the sum of the plasmon resonance of the Au-NPs and the MLCT band of **4** (Figure S3, Supporting Information). Nearly spherical and monodisperse Au-NPs with an average diameter of 4.6 ± 0.7 nm were observed by TEM analysis. TEM images also showed regions in which Au-NPs adopt a hexagonal close-packed (hcp) arrangement (see Figure 2). In these local superstructures, an average distance of 1.7 ± 0.4 nm was measured between Au-NPs. This distance is relatively short in view of the fact that the capping complex **4** contains a dodecyl chain connected to a bulky {(NCS)Fe(salten)} moiety. Such a short distance necessarily implies chain bundles of adjacent iron complexes, highly tilted and/or interdigitated dodecyl chains of neighbouring Au-NPs.^[41]

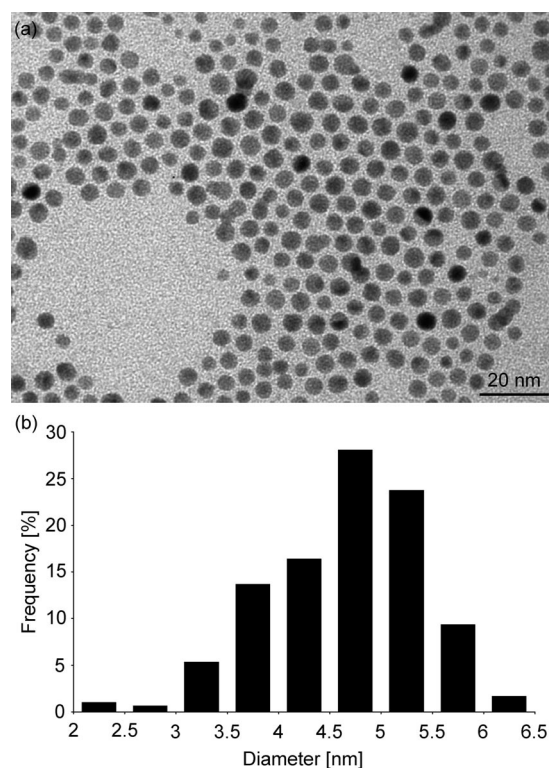


Figure 2. (a) TEM image of Au-NPs functionalized by [(L₄)Fe(NCS)] (**4**) and (b) the corresponding histogram.

Functionalization of Au-NPs by [(L₅)Fe(X)]ⁿ⁺ (X = Solvent Molecule, n = 1; X = NCS⁻, n = 0): Coordination Chemistry on Prefunctionalized NPs

A completely different approach was used to graft the iron complex [(L₅)Fe(X)]ⁿ⁺ (X = solvent molecule, n = 1; X = NCS⁻, n = 0) on Au-NPs. We first changed the type and

the position of the anchoring point, ensuring the connection between the iron complexes and the Au-NPs. The pendant S atom of the isothiocyanato ligand used for complexes **1–4** was replaced by a thiol linker, well-known for its strong affinity for Au surfaces. In addition, this thiol linker was part of the salten derivative ligand L_5 , while in **1–4**, the isothiocyanato ligand was located on the sixth position left available by the salten derivative ligand in the coordination sphere of the iron centre. L_5 was therefore perfectly adapted for a post-functionalization process. The idea was to first stabilize Au-NPs with L_5 and then to insert Fe^{III} into the pendant salten cage of the nanocomposites thus generated.

Au-NPs stabilized by L_5 (AuL_5 -NPs) were obtained through the direct reduction of a mixture of the disulfide $(H_2L_5)_2$ ligand and Au^{III} with excess $NaBH_4$ in dmf. The Au-NPs were purified by repeated precipitations and redispersions (see Experimental Section). The purification process was facilitated by the solubility of the organic ligand in dichloromethane and the insolubility of the functionalized Au-NPs in the same solvent. The purified Au-NPs were finally suspended either in dmf or in a EtOH/ H_2O (v/v, 1:1) mixture. Stable colloidal solutions were obtained in dmf, while partial agglomeration of the nanoparticles was observed in the EtOH/ H_2O mixture. These results were confirmed by UV/Vis spectroscopy. The absorption spectrum of dmf and EtOH/ H_2O solutions showed a single peak in the visible region at 523 nm and 534 nm, respectively (Figure S4, Supporting Information). This band was assigned to the SPR of Au-NPs. The broadening and the red-shift of this SPR band in EtOH/ H_2O relative to dmf were

explained by the partial agglomeration of the Au-NPs in EtOH/ H_2O . Figure 3 shows a TEM image of AuL_5 -NPs, purified and redispersed in dmf. Nearly spherical and monodisperse Au-NPs were observed with a mean diameter of 3.2 ± 0.5 nm. The smaller size obtained for the Au-NPs stabilized with L_5 relative to the ones stabilized with $[(L_4)Fe(NCS)]$ (**4**) can be explained by the stronger interaction of the thiol-terminated ligand L_5 with the gold surface relative to the isothiocyanato pendant group of **4**.

AuL_5 -NPs in dmf and in EtOH/ H_2O were then treated with increasing amounts of $FeCl_3 \cdot 6H_2O$ in order to insert iron(III) centres in the pendant salten cages of the AuL_5 -NPs. The reaction was followed by UV/Vis spectroscopy. When the reaction was carried out in dmf, addition of Fe^{III} led to a slight blueshift from 523 to 517 nm; a slight narrowing and a slight increase in the intensity of the band were observed in the visible region of the spectra (Figure S5, Supporting Information). The slight increase in the intensity of the peak was explained by the addition of the MLCT band of $[(L_5)Fe(solv.)]^+$, centred at 519 nm in the absorption spectrum of pure $[(L_5)Fe(solv.)]^+$, to the SPR band of the Au-NPs. The position of this band led one to assume that the Au-NPs were kept basically unchanged after the insertion of Fe^{III} in the pendant salten cages. This assumption was confirmed by TEM analysis (see Figure 4). Nearly spherical Au-NPs with an average diameter of 3.4 ± 0.5 nm were observed, very close to the size measured for AuL_5 -NPs. Lattice fringes observed in the high-resolution TEM images showed that the majority of the Au-NPs are single crystalline with only a small number of twinned

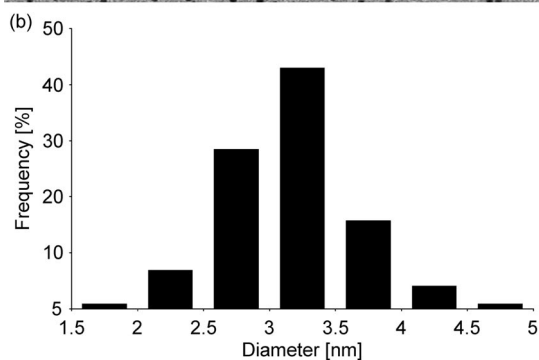
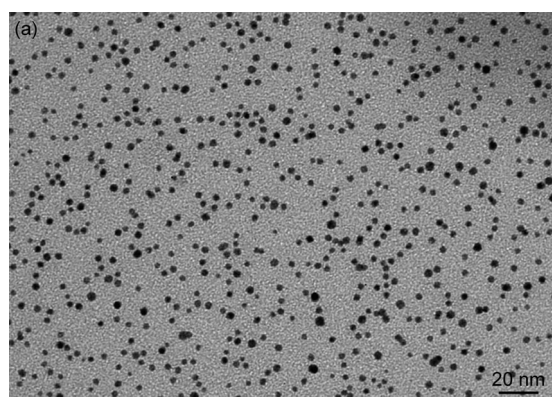


Figure 3. (a) TEM image of Au-NPs functionalized by L_5 in dmf and (b) the corresponding histogram.

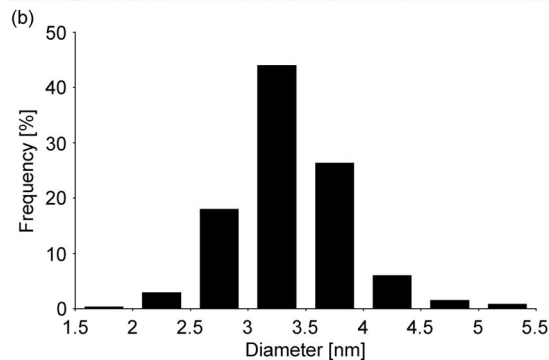
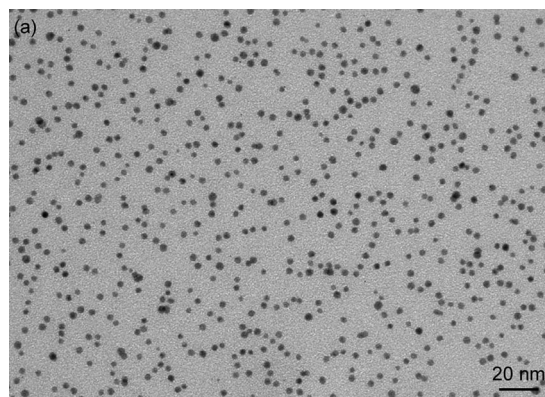


Figure 4. (a) TEM image of AuL_5 -NPs after reaction with Fe^{III} in dmf and (b) the corresponding histogram.

crystals (Figure S6, Supporting Information). When the reaction was performed in EtOH/H₂O, addition of Fe^{III} to preformed AuL₅-NPs significantly altered the electronic spectrum of the colloidal solution. As shown in Figure 5, insertion of Fe^{III} in the pendant salten cages induced a slight increase in the intensity of the band in the visible region, once more explained by the superposition of the MLCT band of [(L₅)Fe(solv.)]⁺ and the SPR band of Au-NPs. Addition of increasing amounts of Fe^{III} also induced a marked narrowing of this band concomitant with a blueshift from 534 nm (0 μL of Fe^{III} solution) to 511 nm (45 μL of Fe^{III} solution, see Experimental Section). Further addition of Fe^{III} did not modify the intensity and the position of the band at 511 nm, implying that all the salten cages were filled. The narrowing and the blueshift can be readily explained by the disassembly of the pristine agglomerated AuL₅-NPs in EtOH/H₂O. Insertion of Fe^{III} in the pendant salten cages of AuL₅-NPs generated charged the capping iron complexes [(L₅)Fe(solv.)]⁺ grafted on the surface of the Au-NPs, and therefore ensured sufficient electrostatic repulsion between nanocomposites to disassemble the original agglomerates. In the final nanocomposites, the sum of the plasmon resonance of the Au-NPs and the MLCT band of [(L₅)Fe(solv.)]⁺ was observed at 511 nm and 517 nm in EtOH/H₂O and in dmf, respectively. This shift could be attributed to the difference in the refractive index of the solvent used in this study ($n_d^{20} = 1.333, 1.361$ and 1.431 for H₂O, EtOH and dmf, respectively). A redshift is actually expected when the refractive index of the solvent increases.^[42]

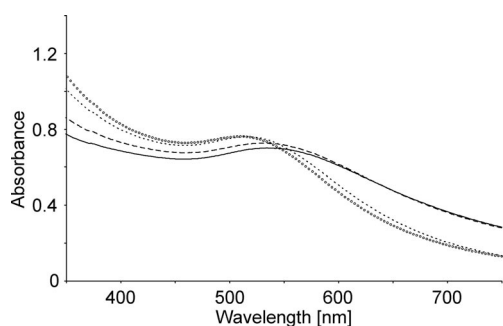


Figure 5. Absorption spectra following the reaction of AuL₅-NPs with increasing amounts of Fe^{III} (see Experimental Section for further details) in EtOH/H₂O. 0 μL (solid line), 15 μL (dashed line), 30 μL (dotted line), 45 μL (empty circles).

The crucial role of electrostatic repulsions in obtaining stable colloidal solutions was further evidenced by the following experiment. Excess ammonium thiocyanate was treated with a stable colloidal solution of Au-NPs functionalized by [(L₅)Fe(solv.)]⁺ in EtOH/H₂O. Thiocyanate was used to replace the solvent molecule in the coordination sphere of the iron complex to generate the neutral complex [(L₅)Fe(NCS)]. Addition of thiocyanate rapidly induced aggregation and precipitation of the nanocomposites as a consequence of the neutralization of the surface charge (Figure S7, Supporting Information). Aggregation of the Au-NPs was also monitored by UV/Vis spectroscopy (Fig-

ure 6). The redshift and the broadening of the SPR band observed in the absorption spectrum were indeed explained by the aggregation phenomenon and thus the delocalization of the plasmon wave through adjacent Au-NPs.^[43] Alternative explanations could also justify the aggregation of the Au-NPs observed after addition of excess ammonium thiocyanate. (i) Thiocyanate ligands are known to bind to the surface of Au-NPs and could therefore remove the positively charged iron complexes from the surface of the Au-NPs and thus induce the aggregation of the Au-NPs. Nevertheless, the affinity of thiocyanate for the surface of Au-NPs is much weaker than the affinity of thiol groups, such as the one used in ligand L₅, for the surface of Au-NPs. The following experiment was realized in order to rule out this conceivable explanation: excess ammonium thiocyanate was added to a stable colloidal solution of Au-NPs functionalized by ligand L₅. No aggregation of the functionalized AuL₅-NPs was observed after addition of this excess ammonium thiocyanate. The place-exchange reaction between [(L₅)Fe(solv.)]⁺ and NCS⁻ can not, therefore, account for the aggregation observed in our initial experiment. (ii) A simple change in the ionic strength of the solution after addition of the excess ammonium thiocyanate could also explain the aggregation observed. Excess ammonium nitrate was therefore added to a stable colloidal solution of Au-NPs functionalized by [(L₅)Fe(solv.)]⁺ in EtOH/H₂O. A small amount of precipitate was observed after several minutes, which showed that modification of the ionic strength partly explains the aggregation observed but can not account for the rapid and complete aggregation observed in our initial experiment, after addition of excess ammonium thiocyanate.

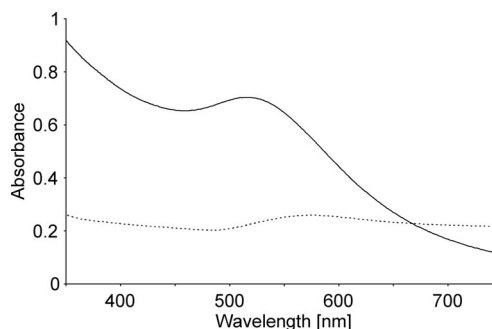


Figure 6. Absorption spectra of preformed Au-NPs functionalized by [(L₅)Fe(solv.)]⁺ in EtOH/H₂O before (solid line) and after (dotted line) addition of excess NH₄NCS.

Conclusions

We have successfully developed different approaches to stabilize and functionalize gold nanoparticles by a new class of iron species, namely salten derivatives of iron(III) complexes. We have been able to vary the nature of the anchoring point between the iron complex and the Au-NP (thiol or thiocyanate), the relative position of this bridging unit in the iron complex [directly connected to the iron(III) cen-

tre or attached to the salten derivative ligand] and the route used for grafting the iron complex on the Au-NPs (direct synthesis or coordination chemistry on prefunctionalized Au-NPs). Steric and electrostatic repulsions have been used to obtain stable colloidal solutions in water and in organic solvents. Such a variety of adaptable parameters of synthesis gives great flexibility to envision the functionalization of metal NPs by numerous iron and other metal complexes derived from Schiff base ligands. This work will indeed be extended to metal Schiff base complexes with specific magnetic properties. For example, it is well-known that the spin-crossover properties can be modulated by the 3D packing of the individual complexes.^[36] Spin-crossover metal complexes will therefore be confined around metal NPs, as only capping components or diluted by magnetically neutral alkylthiol, in order to analyze the influence of the metal NPs on their magnetic properties.

Experimental Section

All reagents and solvents were purchased from Aldrich and used without further purification. H_2 salten (H_2L_1),^[26] H_2 mesalten (H_2L_2),^[44] 4,4'-dithiobis(benzyl alcohol)^[45] and 4,4'-dithiobis(benzyl chloride)^[46] were synthesized by following procedures previously reported, without modification and with similar yields. ESI-MS measurements were carried out with an API 3000 (ESI/MS/MS) PE-SCIEX triple quadrupole mass spectrometer and a HP 5989B single quadrupole mass spectrometer equipped with an electrospray source from Analytica of Branford. For the API 3000 (ESI/MS/MS) PE-SCIEX triple quadrupole mass spectrometer, the experiments were performed either by direct infusion with a syringe pump (with a flow rate of $10 \mu\text{L min}^{-1}$) or by flow injection acquisition (with a flow rate of $200 \mu\text{L min}^{-1}$). Standard experimental conditions were as follows: sample concentration: 10^{-3} to $10^{-5} \text{ mol L}^{-1}$, nebulizing gas N_2 : 7 units flow rate, ion spray voltage: -5.00 kV , temperature: $200\text{--}400 \text{ }^\circ\text{C}$, declustering potential: -20 V , focusing potential: -200 V , entrance potential: 10 V . IR spectra ($4000\text{--}250 \text{ cm}^{-1}$) were recorded with a Nicolet Magna 550 spectrometer (from KBr pellets). Magnetization studies were carried out on a pellet of ground crystals by using a Quantum Design MPMS 5 magnetometer working in the dc mode in the temperature range $300 \text{ K--}5 \text{ K}$ within a magnetic field of 0.5 T and a sweeping rate of 1 K min^{-1} . UV/Vis spectra were recorded with a Perkin-Elmer UV/Vis/NIR lambda 19 PC scanning spectrophotometer. Each colloidal solution was analyzed similarly, being introduced directly from the mother solution into the cell (optical path of 0.2 cm). ^1H and ^{13}C NMR spectra were obtained at room temperature in 5 mm-o.d. tubes with a Bruker Avance 300 spectrometer equipped with a QNP probe head. The following standard abbreviations are used for the characterization of ^1H NMR signals: s = singlet, d = doublet, t = triplet, quin = quintet, m = multiplet, dd = doublet of doublet, td = triplet of doublet. Elemental analyses were realized by the "Service central d'analyse du CNRS", Vernaison (France). Energy-dispersive spectrometry was performed with a PGT-IMIX-PC, and the visualization of metal nanoparticles was performed with a Transmission Electron Microscope (microscope JEOL 2010 UHR and JEOL 100 CX2) in the "Centre Régional de Mesures Physiques" Paris 6: the visualization was performed by drying a drop of the mother solution on a copper grid.

Bis(3-salicylideneaminopropyl)tolylamine, (H_2 tolylsalten, H_2L_3): 4-methylbenzyl bromide ($279 \mu\text{L}$, 2 mmol) and H_2L_1 (0.679 g ,

2 mmol) were solubilized in acetonitrile (60 mL). K_2CO_3 (1.65 g , 12 mmol) and KI (0.100 g , 0.6 mmol) were then added, and the resulting mixture was heated at reflux overnight. After filtration, the solvent was removed under vacuum. The crude ligand was isolated as a yellow oil in 86% yield and was treated with iron(III) without further purification. ^1H NMR (300 MHz , $CDCl_3$, $25 \text{ }^\circ\text{C}$): $\delta = 1.91$ (quin, $J = 6.7 \text{ Hz}$, 4 H , $CH_2\text{--}CH_2\text{--}CH_2$), 2.37 (s, 3 H , CH_3), 2.57 [t, $J = 6.7 \text{ Hz}$, 4 H , $CH_2\text{--}N(CH_2)_2$], 3.58 (s, 2 H , $N\text{--}CH_2\text{--}Ph$), 3.65 (t, $J = 6.6 \text{ Hz}$, 4 H , $C=N\text{--}CH_2$), 6.75 (t, $J = 7.5 \text{ Hz}$, 2 H , $H_{\text{arom}} HC=C\text{--}OH$), 6.84 (d, $J = 8.3 \text{ Hz}$, 2 H , $H_{\text{arom}} N=CH\text{--}C\text{--}CH$), 6.99 (d, $J = 7.7 \text{ Hz}$, 2 H , $H_{\text{arom}} tolyl$), $7.07\text{--}7.11$ (m, 4 H , H_{arom}), 7.18 (d, $J = 7.9 \text{ Hz}$, 2 H , $H_{\text{arom}} tolyl$), 8.13 (s, 2 H , $CH=N$), 13.60 (br. s, 2 H , OH) ppm. ESI-MS (negative ion mode): calcd. for $[H_2L_3 - H]$ 442.3 ; found 442.2 .

Bis(3-salicylideneaminopropyl)dodecylamine, (H_2 dodecansalten, H_2L_4): 1-Bromododecane ($560 \mu\text{L}$, 2 mmol), K_2CO_3 (1.65 g , 12 mmol) and KI (0.100 g , 0.6 mmol) were added to a solution of H_2L_1 (0.644 g , 1.9 mmol) in butanone (60 mL). The resulting mixture was heated at reflux overnight. After removal of the solvent under vacuum, the residue was purified by column chromatography (SiO_2): dichloromethane was used as first eluant to remove unreacted bromododecane, while AcOEt was used to recover the pure product. H_2L_4 was isolated as a yellowish oil in 45% yield (0.460 g). ^1H NMR (300 MHz , $CDCl_3$, $25 \text{ }^\circ\text{C}$): $\delta = 0.93$ (t, $J = 6.9 \text{ Hz}$, 3 H , CH_3), 1.30 (m, 20 H , CH_2), 1.89 (quin, $J = 6.9 \text{ Hz}$, 4 H , $CH_2\text{--}CH_2\text{--}CH_2$), 2.45 (t, $J = 7.1 \text{ Hz}$, 2 H , $N\text{--}CH_2$ from $C_{12}H_{25}$), 2.58 [t, $J = 6.9 \text{ Hz}$, 4 H , $CH_2\text{--}N(CH_2)_2$], 3.66 (t, $J = 6.7 \text{ Hz}$, 4 H , $C=N\text{--}CH_2$), 6.90 (t, $J = 7.5 \text{ Hz}$, 2 H , $H_{\text{arom}} HC=C\text{--}OH$), 7.00 (d, $J = 5.6 \text{ Hz}$, 2 H , $H_{\text{arom}} N=CH\text{--}C\text{--}CH$), 7.25 (dd, $J = 1.3$, $J = 7.5 \text{ Hz}$, 2 H , H_{arom}), 7.34 (td, $J = 8.7$, $J = 1.5 \text{ Hz}$, 2 H , H_{arom}), 8.37 (s, 2 H , $CH=N$), 13.60 (s, 2 H , OH) ppm. ^{13}C NMR (75 MHz , $CDCl_3$, $25 \text{ }^\circ\text{C}$): $\delta = 14.2$ (CH_3), 22.7 ($CH_3\text{--}CH_2$), 27.2 , 27.7 , 28.5 , 29.4 , 29.7 , 29.74 , 32.0 , 51.4 [$N\text{--}(CH_2)_2$], 54.1 ($N\text{--}CH_2$), 57.5 ($C=N\text{--}CH_2$), 117.0 ($CH=C\text{--}OH$), 118.5 ($C\text{--}C=N$), 188.8 ($CH=CH\text{--}C=N$), 131.1 ($CH=CH\text{--}C=N$), 132.1 ($CH=CH\text{--}C\text{--}OH$), 161.4 ($C\text{--}OH$), 164.9 ($C=N$) ppm. ESI-MS (positive ion mode): calcd. for $[H_2L_4 + H]$ 508.4 ; found 508.6 .

Bis(3-salicylideneaminopropyl)-*p*-tolylthiolamine [(H_2 tolylthiol-salten) $_2$, (H_2L_5) $_2$]: K_2CO_3 (1.65 g , 12 mmol) and KI (0.100 g , 0.6 mmol) were added to a solution of 4,4'-dithiobis(benzyl chloride) (0.516 g , 1.5 mmol) in acetonitrile (240 mL). H_2L_1 (1 g , 3 mmol) was then added, and the resulting mixture was heated at reflux overnight. After filtration, the solvent was removed under vacuum and the product was purified by flash chromatography (SiO_2 , AcOEt). (H_2L_5) $_2$ was isolated as a yellow oil in 91% yield (1.26 g). ^1H NMR (300 MHz , $CDCl_3$, $25 \text{ }^\circ\text{C}$): $\delta = 1.87$ (quin, $J = 7.0 \text{ Hz}$, 8 H , $CH_2\text{--}CH_2\text{--}CH_2$), 2.59 [t, $J = 7.0 \text{ Hz}$, 8 H , $CH_2\text{--}N(CH_2)_2$], 3.64 (t, $J = 6.1 \text{ Hz}$, 8 H , $C=N\text{--}CH_2$), 3.69 (s, 4 H , $CH_2\text{--}Ph$), 6.82 (t, $J = 7.9 \text{ Hz}$, 4 H , $H_{\text{arom}} CH=C\text{--}OH$), 6.92 (d, $J = 8.8 \text{ Hz}$, 4 H , $H_{\text{arom}} thiophenol$), 7.11 (t, $J = 7.9 \text{ Hz}$, 6 H) $7.20\text{--}7.31$ (m, 6 H), 7.64 (dd, $J = 7.0$, $J = 1.7 \text{ Hz}$, 4 H), 8.3 (s, 4 H , $CH=N$), 13.5 (s, 4 H , OH) ppm. ^{13}C NMR (75 MHz , $CDCl_3$, $25 \text{ }^\circ\text{C}$): $\delta = 27.9$ ($CH_2\text{--}CH_2\text{--}CH_2$), 50.8 ($N\text{--}CH_2\text{--}CH_2\text{--}CH_2$), 57.5 ($CH_2\text{--}CH_2\text{--}N=C$), 58.4 ($N\text{--}CH_2\text{--}Ph$), 117.0 ($CH=C\text{--}OH$), 117.7 ($C=C=N$), 118.4 ($CH=CH\text{--}C=N$), 126.3 ($S=C\text{--}CH\text{--}CH=C$), 128.6 ($S=C\text{--}CH\text{--}CH=C$), 129.9 ($CH\text{--}C\text{--}C=N$), 131.2 ($CH=CH\text{--}C\text{--}OH$), 137.9 ($S=C\text{--}CH\text{--}CH=C$), 138.3 ($C\text{--}S$), 161.3 ($C\text{--}OH$), 164.9 ($C=N$) ppm. ESI-MS (negative ion mode): calcd. for $[(H_2L_5)_2 - H]$ 920.2 ; found 919.9 , calcd. for $[(H_2L_5)_2 - 2H]$ 459.6 ; found 460.6 .

[(L_1)Fe(NCS)] (1), [(L_2)Fe(NCS)] (2), [(L_3)Fe(NCS)] (3), [(L_4)Fe(NCS)] (4) and [(L_5)Fe(NCS)] $_2$: The five complexes were synthesized by following similar procedures. $Fe(NO_3)_3 \cdot 9H_2O$ (0.404 g ,

1 mmol) and NH_4NCS (0.457 g, 6 mmol) were solubilized in ethanol (50 mL) to give solution S_1 . The appropriate salen derivative ligand [H_2L_1 : 0.339 g, 1 mmol; H_2L_2 : 0.353 g, 1 mmol; H_2L_3 : 0.444 g, 1 mmol; H_2L_4 : 0.508 g, 1 mmol; (H_2L_5)₂: 0.461 g, 0.5 mmol] and NaOCH_3 (0.108 g, 2 mmol) were mixed together in ethanol (50 mL), or in butanone for H_2L_4 , to give solution S_2 . Solution S_1 was then slowly added to solution S_2 , and the resulting solution was stirred at room temperature for 30 min. Crystals of **1**, **2** and **3** were obtained by slow evaporation of the solvent. Yields of about 40% were obtained for the three complexes. For [L_4]- $\text{Fe}(\text{NCS})$ (**4**), the solution was concentrated to ca. 50 mL. Complex **4** was recovered after extraction with a mixture of diethyl ether (2×100 mL) and water (2×20 mL). The organic phases were then combined, dried with MgSO_4 , and the solvent was evaporated to afford **4** (80% yield). [L_5] $\text{Fe}(\text{NCS})_2$ precipitated from the solution by slow evaporation of the solvent (95% yield). [L_1] $\text{Fe}(\text{NCS})$ (**1**): $\text{C}_{21}\text{H}_{23}\text{FeN}_4\text{O}_2\text{S}$ (451.34): calcd. C 55.88, H 5.14, Fe 12.37, N 12.41, S 7.10; found C 55.27, H 5.09, Fe 12.15, N 12.44, S 6.72. IR (KBr): $\tilde{\nu} = 3236$ (w, NH), 2053 (vs, CN thiocyanate), 1622 (vs, CN imine), 1597 (s), 1542 (s), 1468 (s), 1444 (s), 1401 (m), 1387 (m), 1335 (m), 1304 (s, CO), 1204 (m), 1149 (m), 1089 (m), 1048 (m), 887 (m), 787 (m), 778 (m), 754 (m), 431 (m), 276 (m) cm^{-1} . UV/Vis (dmf): λ (ϵ / $\text{L mol}^{-1} \text{cm}^{-1}$) = 513 (3200), 402 (sh, 2895), 329 (7870), 298 (sh, 5815) nm. ESI-MS (positive ion mode): calcd. for $[\text{M} - \text{NCS}]^+$ 393.2; found 393.3. [L_2] $\text{Fe}(\text{NCS})$ (**2**): $\text{C}_{22}\text{H}_{25}\text{FeN}_4\text{O}_2\text{S}$ (465.4): calcd. C 56.78, H 5.41, Fe 12.00, N 12.04, S 6.89; found C 56.64, H 5.43, Fe 11.73, N 12.11, S 6.49. IR (KBr): $\tilde{\nu} = 2917$ (w), 2890 (w), 2865 (w), 2062 (vs, CN thiocyanate), 1620 (vs, CN imine), 1598 (s), 1540 (s), 1467 (s), 1443 (s), 1398 (m), 1305 (s, CO), 1148 (m), 761 (s), 594 (m), 440 (m) cm^{-1} . UV/Vis (dmf): λ (ϵ / $\text{L mol}^{-1} \text{cm}^{-1}$) = 512 (2645), 406 (sh, 3310), 323 (10425), 296 (sh, 8900) nm. ESI-MS (positive ion mode): calcd. for $[\text{M} - \text{NCS}]^+$ 407.3; found 407.3. [L_3] $\text{Fe}(\text{NCS})$ (**3**): $\text{C}_{29}\text{H}_{31}\text{FeN}_4\text{O}_2\text{S}$ (555.49): calcd. C 62.71, H 5.63, Fe 10.05, N 10.09, S 5.77; found C 62.35, H 5.71, Fe 9.98, N 9.93, S 5.31. IR (KBr): $\tilde{\nu} = 2921$ (m), 2897 (m), 2057 (vs, CN thiocyanate), 1620 (vs, CN imine), 1541 (vs), 1466 (s), 1444 (vs), 1395 (m), 1340 (m), 1301 (s, CO), 1201 (m), 1148 (m), 1124 (m), 1090 (m), 1047 (m), 757 (s), 742 (m), 596 (s), 451 (m), 431 (m) cm^{-1} . UV/Vis (dmf): λ (ϵ / $\text{L mol}^{-1} \text{cm}^{-1}$) = 508 (3940),

332 (12110), 296 (sh, 9185) nm. ESI-MS (positive ion mode): calcd. for $[\text{M} - \text{NCS}]^+$ 497.4; found 497.3. [L_4] $\text{Fe}(\text{NCS})$ (**4**): IR (KBr): $\tilde{\nu} = 2922$ (s), 2852 (s), 2052 (vs, CN thiocyanate), 1647 (m), 1619 (s, CN imine), 1544 (s), 1469 (s), 1446 (s), 1309 (m, CO), 1150 (m), 758 (m) cm^{-1} . ESI-MS (positive ion mode): calcd. for $[\text{M} - \text{NCS}]^+$ 561.6; found 561.4. [L_5] $\text{Fe}(\text{NCS})_2$: ESI-MS (positive ion mode): calcd. for $[\text{M} - \text{NCS}]^+$ 1087.0; found 1086.6.

Au-NPs Coated by 1, 2 and 3: Syntheses of the nanocomposites were identical with those of the three iron complexes. The ratio $[\text{Au}^{\text{III}}]/[\text{Fe}^{\text{III}}]$ was varied between 0.25 and 6 without noticeable influence on the final size and shape of the nanocomposites. In a typical experiment, a dmf solution (2 mL) of $\text{HAuCl}_4 \cdot 3\text{H}_2\text{O}$ (5.8 mg, 0.015 mmol) was added to a solution of **1** (6.8 mg, 0.015 mmol) in dmf (8 mL). An aqueous solution of NaBH_4 (0.140 mL, 0.4 M) was then added at once to the previous mixture. The resulting solution was stirred for 15 min at room temperature. The solution was analyzed by UV/Vis spectroscopy and TEM.

Au-NPs Stabilized by 4: A dmf solution (2 mL) of $\text{HAuCl}_4 \cdot 3\text{H}_2\text{O}$ (5.8 mg, 0.015 mmol) and an aqueous solution of NaBH_4 (0.140 mL, 0.4 M) were successively added, at once, to a solution of **4** (9.3 mg, 0.015 mmol) in dmf (8 mL). The resulting solution was stirred 15 min at room temperature. The dark red colloidal solution was then repeatedly centrifuged for 20 min at 14000 rpm at 5 °C, and the nanocomposites were redispersed in dmf (10 mL) in order to remove excess **4**.

Au-NPs Stabilized by L_5 : A solution of (H_2L_5)₂ in dichloromethane (0.130 mL, 0.11 M) was poured into dmf (8 mL). To this solution were then successively added a solution of $\text{HAuCl}_4 \cdot 3\text{H}_2\text{O}$ (5.8 mg, 0.015 mmol) in dmf (2 mL) and an aqueous solution of NaBH_4 (0.140 mL, 0.4 M). The resulting red solution was stirred for 15 min at room temperature. The AuL_5 -NPs were then purified from free organic ligands by using the following protocol. A mixture of dichloromethane (60 mL) and water (5 mL) was added to the previous stable colloidal solution. AuL_5 -NPs precipitated, while the non-grafted organic ligands remained in solution. The precipitate was then recovered by centrifugation and redispersed in dmf (10 mL). The above treatment was then repeated in order to remove traces of free (H_2L_5)₂. Purified AuL_5 -NPs were finally redispersed

Table 2. Crystallographic data for [L_1] $\text{Fe}(\text{NCS})$ (**1**), [L_2] $\text{Fe}(\text{NCS})$ (**2**) and [L_3] $\text{Fe}(\text{NCS})$ (**3**).

	[L_1] $\text{Fe}(\text{NCS})$ (1)	[L_2] $\text{Fe}(\text{NCS})$ (2)	[L_3] $\text{Fe}(\text{NCS})$ (3)
Empirical formula	$\text{C}_{21}\text{H}_{23}\text{FeN}_4\text{O}_2\text{S}$	$\text{C}_{22}\text{H}_{25}\text{FeN}_4\text{O}_2\text{S}$	$\text{C}_{29}\text{H}_{31}\text{FeN}_4\text{O}_2\text{S}$
Formula weight	451.34	465.37	555.49
Crystal system	orthorhombic	orthorhombic	monoclinic
Space group	<i>Pna</i> 2 ₁	<i>Pbca</i>	<i>P2₁/n</i>
<i>T</i> [K]	293(2)	296(2)	293(2)
<i>a</i> [Å]	13.5764(6)	12.9976(3)	10.1055(3)
<i>b</i> [Å]	16.6768(7)	16.7318(4)	15.1459(4)
<i>c</i> [Å]	9.3723(3)	20.2176(4)	17.5384(6)
α [°]	90	90	90
β [°]	90	90	92.623(2)
γ [°]	90	90	90
<i>V</i> [Å ³]	2121.99(15)	4396.79(17)	2681.56(14)
<i>Z</i>	4	8	4
ρ_{calcd} [g cm ⁻³]	1.413	1.406	1.376
μ [mm ⁻¹]	0.833	0.807	0.674
<i>F</i> (000)	940	1944	1164
Reflections collected	19896	83482	67913
Independent reflections	6026 ($R_{\text{int}} = 0.0357$)	6446 ($R_{\text{int}} = 0.0528$)	7847 ($R_{\text{int}} = 0.0362$)
Goodness-of-fit on F^2	1.022	1.095	1.079
R_1, wR_2 [$I > 2\sigma(I)$]	0.0371, 0.0832	0.0361, 0.1008	0.0407, 0.1125
R_1, wR_2 [all data]	0.0702, 0.0962	0.0830, 0.1365	0.0576, 0.1233
$\Delta\rho(\text{max}), \Delta\rho(\text{min})$ [e Å ⁻³]	0.379, -0.338	0.649, -0.721	0.467, -0.330

either in dmf (10 mL), in which case the solution was denoted S_{dmf} , or in a mixture of ethanol (5 mL) and water (5 mL), in which case the solution was denoted S_{aq} .

Reactivity of AuL₅-NPs with Fe^{III}: Portions (0.015 mL) of solutions of FeCl₃·6H₂O in dmf (0.04 M) and in EtOH/H₂O (v/v, 1:1, 0.02 M) were added to S_{dmf} and S_{aq} , respectively. The reaction of complexation was followed by UV/Vis spectroscopy.

X-ray Diffraction Analyses: X-ray intensity data were collected with a Bruker X8-APEX2 CCD area-detector diffractometer by using Mo- K_{α} radiation ($\lambda = 0.71073 \text{ \AA}$). Three sets of narrow data frames (90 s per frame) for **1**, four sets of narrow data frames (240 s per frame) for **2**, and six sets of narrow data frames (30 s per frame) for **3** were collected at different values of θ , for two and one initial values of ϕ and ω , respectively, for **1** (two and two initial values for **2** and three and three initial values for **3**), by using 0.5° increments of ϕ and ω . Data reduction was accomplished with SAINT, v7.03.^[47] The substantial redundancy in data (4.56 for **1**, 9.37 for **2** and 6.46 for **3**) allowed a semiempirical absorption correction (SADABS v2.10)^[47] to be applied on the basis of multiple measurements of equivalent reflections. The structure was solved by direct methods, developed by successive different Fourier syntheses and refined by full-matrix least-squares on all F^2 data by using SHELXTL v6.14.^[48] Hydrogen atoms were included in calculated positions and allowed to ride on their parent atoms. The crystallographic data are summarized in Table 2.

CCDC-678513 (for **1**), -678514 (for **2**) and -678512 (for **3**) contain the supplementary crystallographic data for this paper. These data can be obtained free of charge from The Cambridge Crystallographic Data Centre via www.ccdc.cam.ac.uk/data_request/cif.

Supporting Information (see footnote on the first page of this article): Thermal dependence curve of χ_{MT} for **3**, absorption spectra of functionalized Au-NPs, HRTEM image of AuL₅-NPs and picture showing the influence of the addition of NCS⁻ to a stable colloidal solution of Au-NPs functionalized by [(L₅)Fe(sol_v.)]⁺.

Acknowledgments

We thank Dr. L. Catala for magnetic measurements. This work has been supported by the Région Île-de-France in the framework of C'nano ÎdF. C'Nano-ÎdF is the nanoscience competence centre of the Paris Region, supported by CNRS, CEA, MESR and Région Île-de-France. This work was also supported by a grant from the French Agence Nationale de la Recherche (ANR-07-JCJC-0040).

- [1] P. Migowski, J. Dupont, *Chem. Eur. J.* **2007**, *13*, 32–39.
 [2] R. W. J. Scott, O. M. Wilson, R. M. Crooks, *J. Phys. Chem. B* **2005**, *109*, 692–704.
 [3] a) E. Katz, I. Willner, *Angew. Chem. Int. Ed.* **2004**, *43*, 6042–6108; b) N. L. Rosi, C. A. Mirkin, *Chem. Rev.* **2005**, *105*, 1547–1562.
 [4] J. D. E. T. Wilton-Ely, *Dalton Trans.* **2008**, 25–29.
 [5] a) Y. Kim, R. C. Johnson, J. T. Hupp, *Nano Lett.* **2001**, *1*, 165–167; b) C.-C. Huang, H.-T. Chang, *Chem. Commun.* **2007**, 1215–1217.
 [6] C.-C. Huang, Z. Yang, K.-H. Lee, H.-T. Chang, *Angew. Chem. Int. Ed.* **2007**, *46*, 6824–6828.
 [7] K. Yoosaf, B. I. Ipe, C. H. Suresh, K. G. Thomas, *J. Phys. Chem. C* **2007**, *111*, 12839–12847.
 [8] B. I. Ipe, K. Yoosaf, K. G. Thomas, *J. Am. Chem. Soc.* **2006**, *128*, 1907–1913.
 [9] a) T. B. Norsten, B. L. Frankamp, V. M. Rotello, *Nano Lett.* **2002**, *2*, 1345–1348; b) X. Zhang, D. Li, X.-P. Zhou, *New J. Chem.* **2006**, *30*, 706–711.
 [10] a) Y. Kuwahara, T. Akiyama, S. Yamada, *Langmuir* **2001**, *17*, 5714–5716; b) P. Pramod, P. K. Sudeep, K. G. Thomas, P. V. Kamat, *J. Phys. Chem. B* **2006**, *110*, 20737–20741; c) W. Huang, G. Masuda, S. Maeda, H. Tanaka, T. Hino, T. Ogawa, *Inorg. Chem.* **2008**, *47*, 468–480.
 [11] C. R. Mayer, E. Dumas, F. Miomandre, R. Méallet-Renault, F. Warmont, J. Vigneron, R. Pansu, A. Etcheberry, F. Sécheresse, *New J. Chem.* **2006**, *30*, 1628–1637.
 [12] M. Jebb, P. K. Sudeep, P. Pramod, K. G. Thomas, P. V. Kamat, *J. Phys. Chem. B* **2007**, *111*, 6839–6844.
 [13] a) J. Wang, J. Li, A. J. Baca, J. Hu, F. Zhou, W. Yan, D. W. Pang, *Anal. Chem.* **2003**, *75*, 3941–3945; b) M. Yamada, H. Nishihara, *Langmuir* **2003**, *19*, 8050–8056; c) R. L. Wolfe, R. Balasubramanian, J. B. Tracy, R. W. Murray, *Langmuir* **2007**, *23*, 2247–2254.
 [14] D. Astruc, M.-C. Daniel, J. Ruiz, *Chem. Commun.* **2004**, 2637–2649.
 [15] F. S. Nunes, L. D. S. Bonifacio, K. Araki, H. E. Toma, *Inorg. Chem.* **2006**, *45*, 94–101.
 [16] S. H. Toma, J. A. Bonacin, K. Araki, H. E. Toma, *Eur. J. Inorg. Chem.* **2007**, 3356–3364.
 [17] a) S. S. Kumar, J. Joseph, K. L. Phani, *Chem. Mater.* **2007**, *19*, 4722–4730; b) J. D. Qiu, H. Z. Peng, R. P. Liang, J. Li, X. H. Xia, *Langmuir* **2007**, *23*, 2133–2137.
 [18] J. R. Aranzaes, C. Belin, D. Astruc, *Chem. Commun.* **2007**, 3456–3458.
 [19] J. Jullien, G. Juhasz, P. Mialane, E. Dumas, C. R. Mayer, J. Marrot, E. Riviere, E. L. Bominaar, E. Munck, F. Secheresse, *Inorg. Chem.* **2006**, *45*, 6922–6927.
 [20] G. Rogez, A. Marvilliers, E. Rivière, J.-P. Audière, F. Lloret, F. Varret, A. Goujon, N. Mendenez, J.-J. Girerd, T. Mallah, *Angew. Chem. Int. Ed.* **2000**, *39*, 2885–2887.
 [21] G. Rogez, A. Marvilliers, P. Sarr, S. Parsons, S. J. Teat, L. Ricard, T. Mallah, *Chem. Commun.* **2002**, 1460–1461.
 [22] G. Rogez, S. Parsons, C. Paulsen, V. Villar, T. Mallah, *Inorg. Chem.* **2001**, *40*, 3836–3837.
 [23] a) A. Ohyoshi, J. Honbo, N. Matsumoto, S. Ohta, S. Sakamoto, *Bull. Chem. Soc. Jpn.* **1986**, *59*, 1611–1613; b) Y. Maeda, M. Suzuki, S. Hirose, S. Hayami, T. Oniki, S. Sugihara, *Bull. Chem. Soc. Jpn.* **1998**, *71*, 2837–2843; c) A. Sour, M.-L. Boillot, E. Rivière, P. Lesot, *Eur. J. Inorg. Chem.* **1999**, 2117–2119.
 [24] S. Hirose, S. Hayami, Y. Maeda, *Bull. Chem. Soc. Jpn.* **2000**, *73*, 2059–2066.
 [25] C. Faulmann, S. Dorbes, B. Garreau de Bonneval, G. Molnár, A. Bousseksou, C. J. Gomez-Garcia, E. Coronado, L. Valade, *Eur. J. Inorg. Chem.* **2005**, 3261–3270.
 [26] N. Matsumoto, S. Ohta, C. Yoshimura, A. Ohyoshi, S. Kohata, H. Okawa, Y. Maeda, *J. Chem. Soc., Dalton Trans.* **1985**, 2575–2584.
 [27] a) S. Ohta, C. Yoshimura, N. Matsumoto, H. Okawa, A. Ohyoshi, *Bull. Chem. Soc. Jpn.* **1986**, *59*, 155–159; b) S. Hayami, Y. Hosokoshi, K. Inoue, Y. Einaga, O. Sato, Y. Maeda, *Bull. Chem. Soc. Jpn.* **2001**, *74*, 2361–2368.
 [28] C. R. Mayer, E. Dumas, F. Sécheresse, *Chem. Commun.* **2005**, 345–347.
 [29] C. R. Mayer, E. Dumas, A. Michel, F. Sécheresse, *Chem. Commun.* **2006**, 4183–4185.
 [30] a) T. Yonezawa, K. Yasui, N. Kimizuka, *Langmuir* **2001**, *17*, 271–273; b) C. S. Love, V. Chechik, D. K. Smith, C. Brennan, *J. Mater. Chem.* **2004**, *14*, 919–923.
 [31] P. Ionita, A. Carageorghopol, B. C. Gilbert, V. Chechik, *J. Am. Chem. Soc.* **2002**, *124*, 9048–9049.
 [32] K. Tanimura, R. Kitashima, N. Bréfuel, M. Nakamura, N. Matsumoto, S. Shova, J.-P. Tuchagues, *Bull. Chem. Soc. Jpn.* **2005**, *78*, 1279–1282.
 [33] Y. Maeda, Y. Noda, H. Oshio, Y. Takashima, *Bull. Chem. Soc. Jpn.* **1992**, *65*, 1825–1831.
 [34] X. Wang, M. E. Kotun, W. T. Pennington, J. C. Fanning, *Inorg. Chim. Acta* **1988**, *154*, 189–199.

- [35] E. Sinn, G. Sim, E. V. Dose, M. F. Tweedle, L. J. Wilson, *J. Am. Chem. Soc.* **1978**, *100*, 3375–3390.
- [36] S. Floquet, M. C. Munoz, E. Riviere, R. Clement, J.-P. Audiere, M.-L. Boillot, *New J. Chem.* **2004**, *28*, 535–541.
- [37] a) J.-L. Yao, X. Xu, D.-Y. Wu, Y. Xie, B. Ren, Z.-Q. Tian, G.-P. Pan, D.-M. Sun, K.-H. Xue, *Chem. Commun.* **2000**, 1627–1628; b) J.-Q. Hu, Q. Chen, Z. X. Xie, G. B. Han, R. H. Wang, B. Ren, Y. Zhang, Z. L. Yang, Z. Q. Tian, *Adv. Funct. Mater.* **2004**, *14*, 183–189; c) B. Zhang, J. F. Li, Q. L. Zhong, B. Ren, Z. Q. Tian, S. Z. Zou, *Langmuir* **2005**, *21*, 7449–7455; d) G. Hu, Z. Feng, D. Han, J. Li, G. Jia, J. Shi, C. Li, *J. Phys. Chem. C* **2007**, *111*, 8632–8637; e) G. Hu, Z. Feng, J. Li, G. Jia, D. Han, Z. Liu, C. Li, *J. Phys. Chem. C* **2007**, *111*, 11267–11274.
- [38] a) P. V. Kamat, *J. Phys. Chem. B* **2002**, *106*, 7729–7744; b) W. E. Doering, S. Nie, *Anal. Chem.* **2003**, *75*, 6171–6176; c) D. Cheng, Q.-H. Xu, *Chem. Commun.* **2007**, 248–250.
- [39] C. PerezLeon, L. Kador, B. Peng, M. Thelakkat, *J. Phys. Chem. B* **2005**, *109*, 5783–5789.
- [40] M. Brust, M. Walker, D. Bethell, D. J. Schiffrin, R. Whyman, *J. Chem. Soc., Chem. Commun.* **1994**, 801–802.
- [41] X. Wang, Y. Li, *Chem. Commun.* **2007**, 2901–2910.
- [42] S. Underwood, P. Mulvaney, *Langmuir* **1994**, *10*, 3427–3430.
- [43] S. Zhang, G. Leem, L. Srisombat, T. R. Lee, *J. Am. Chem. Soc.* **2008**, *130*, 113–120.
- [44] B. B. Corden, R. S. Drago, R. P. Perito, *J. Am. Chem. Soc.* **1985**, *107*, 2903–2907.
- [45] R. Grice, L. N. Owen, *J. Chem. Soc.* **1963**, 1947–1954.
- [46] V. I. Dronov, R. F. Nigmatullina, *Russ. Chem. Bull.* **1976**, *25*, 2609–2611.
- [47] APEX2 version 1.0–8; Bruker AXS: Madison, WI, **2003**.
- [48] SHELXTL version 6.14; Bruker AXS: Madison, WI, **2001**.

Received: March 4, 2008
Published Online: July 4, 2008